



OPEN

Upregulation of microRNA-96-5p is associated with adolescent idiopathic scoliosis and low bone mass phenotype

Huanxiong Chen^{1,2,7}, Kenneth Guangpu Yang^{2,7}, Jiajun Zhang^{2,7}, Ka-yee Cheuk^{2,7}, Evguenia Nepotchatykh³, Yujia Wang², Alec Lik-hang Hung², Tsz-ping Lam², Alain Moreau^{3,4,5}✉ & Wayne Yuk-wai Lee^{2,6}✉

Bone densitometry revealed low bone mass in patients with adolescent idiopathic scoliosis (AIS) and its prognostic potential to predict curve progression. Recent studies showed differential circulating miRNAs in AIS but their diagnostic potential and links to low bone mass have not been well-documented. The present study aimed to compare miRNA profiles in bone tissues collected from AIS and non-scoliotic subjects, and to explore if the selected miRNA candidates could be useful diagnostic biomarkers for AIS. Microarray analysis identified miR-96-5p being the most upregulated among the candidates. miR-96-5p level was measured in plasma samples from 100 AIS and 52 healthy girls. Our results showed significantly higher plasma levels of miR-96-5p in AIS girls with an area under the curve (AUC) of 0.671 for diagnostic accuracy. A model that was composed of plasma miR-96-5p and patient-specific parameters (age, body weight and years since menarche) gave rise to an improved AUC of 0.752. Ingenuity Pathway Analysis (IPA) indicated functional links between bone metabolic pathways and miR-96-5p. In conclusion, differentially expressed miRNAs in AIS bone and plasma samples represented a new source of disease biomarkers and players in AIS etiopathogenesis, which required further validation study involving AIS patients of both genders with long-term follow-up.

Adolescent Idiopathic Scoliosis (AIS) is the most common form of three-dimensional spinal deformity in paediatric population, which affects adolescent between 10 and 16 years of age with a global prevalence of 2–4%¹. Due to the unclear etiopathogenesis, the current treatment strategy for AIS is mainly targeting on anatomical abnormality instead of the cause², which often results in suboptimal treatments and psychological sequelae. Therefore, early diagnosis and prediction of curve progression are important research questions to aid patient stratification at earlier stage for more effective and timely treatment.

The observation of discordant curve type and curve severity on monozygotic twins implies the significant role of non-genetic factors in AIS pathogenesis³. In the past decade, genome-wide associations studies (GWAS) have reported hundreds of AIS susceptibility loci⁴. Subsequent functional studies revealed role of these genes in etiopathology of AIS, such as ladybird homeobox 1 (*LBX1*) in paraspinal muscle^{5–8}. More recent studies from literature suggest that epigenetic mechanisms may contribute to etiopathology of AIS⁹, including DNA methylation, long non-coding RNAs (lncRNA) and microRNAs (miRNAs). DNA methylation changes the activity of genes by adding methyl groups to the DNA molecules with the DNA sequences unchanged¹⁰. Methylation of Wnt family member 10A (*WNT10A*)¹¹, neuropeptide Y (*NPY*)¹¹, nestrogen receptor 1 (*ESR1*)¹², estrogen receptor 2 (*ESR2*)¹³,

¹Department of Spine Surgery, The First Affiliated Hospital of Hainan Medical University, Haikou, Hainan, China. ²Department of Orthopaedics and Traumatology, SH Ho Scoliosis Research Laboratory, Joint Scoliosis Research Centre of the Chinese University of Hong Kong and Nanjing University, The Chinese University of Hong Kong, Hong Kong SAR, China. ³Viscogliosi Laboratory in Molecular Genetics of Musculoskeletal Diseases, Sainte-Justine University Hospital Research Center, Montreal, QC, Canada. ⁴Department of Stomatology, Faculty of Dentistry, Université de Montréal, Montreal, QC, Canada. ⁵Department of Biochemistry and Molecular Medicine, Faculty of Medicine, Université de Montréal, Montreal, QC, Canada. ⁶Li Ka Shing Institute of Health Sciences, The Chinese University of Hong Kong, Hong Kong SAR, China. ⁷These authors contributed equally: Huanxiong Chen, Kenneth Guangpu Yang, Jiajun Zhang and Ka-yee Cheuk. ✉email: alain.moreau.hsj@sss.gouv.qc.ca; waynelee@cuhk.edu.hk

	AIS (N = 4, Females)		Non-scoliotic subjects (N = 4, 3 Males and 1 Female)		P value
	Mean	SD	Mean	SD	
Age	15.17	1.60	14.00	3.67	0.580
Standing height (cm)	158.35	5.49	161.63	5.68	0.069
Body weight (kg)	54.23	17.29	53.50	25.30	0.724
Arm span (cm)	158.93	6.38	161.30	6.39	0.275
Cobb angle (°)	48.00	5.89	–	–	–
Tanner stage (pubic hair)	4.00	1.10	3.20	1.64	0.375
Tanner stage (breast)	4.17	0.41	3.80	1.30	0.763

Table 1. Clinical and demographic characteristics of participants involved in discovery cohort.

protocadherin 10 (*PCDH10*)¹⁴, cartilage oligomeric matrix protein (*COMP*)¹⁵, hyaluronan synthase 2 (*HAS2*)¹⁶, pituitary homeobox 1 (*PITX1*)¹⁷, histone H3 lysine 9 (*H3K9*)¹⁸, and necdin (*NDN*)¹⁹ genes were reported to be relevant to AIS. lncRNAs, transcripts longer than 200 nucleotides, do not contain functional open reading frames but regulate gene expression²⁰. H19 lncRNA was reported to be differentially expressed in convex and concave side of paravertebral muscle in AIS²¹. Liu et al. have identified 139 lncRNAs that were differentially expressed in the AIS patients when compared with the controls²². miRNAs are a class of endogenous short noncoding RNAs (~22–26 nucleotides in length) that regulate diverse biological processes²³ through binding to messenger RNA (mRNA) targets. The miRNAs are known to modulate the sporadic and phenotypical alterations by transducing environmental stimuli into biological signaling²⁴. The clinical use of miRNAs is gaining a lot of interests in molecular medicine because they are detectable in many different biological fluids²⁵. Emerging evidence suggest the presence of differential miRNA profile in AIS. Abnormal circulating levels of miR-151a-3p²⁶, miR-30e²⁷, miR-122-5p, miR-27a-5p, miR-223-5p, miR-671-5p and miR1306-3p have been discovered and validated in blood samples from AIS patients in previous case–control studies. Those studies provide strong evidence supporting potential role of epigenetics in AIS²⁸.

Osteopenia, defined as a Z-score of femoral neck areal bone mineral density (aBMD) below –1, was reported in about one third of AIS patients, 80% of which could persist to skeletal maturity^{29–31}. Recent studies with high resolution quantitative computed tomography (HR-pQCT) revealed significant alterations of cortical and trabecular bone qualities in AIS with normal BMD by dual energy X-ray absorptiometry (DXA)^{32,33}. Cortical volumetric BMD (vBMD) at distal radius was found to enhance prediction of curve progression in AIS³⁴. AIS patients had high levels of serum bone turnover markers, and high level of bone turnover in time-lase analysis of local bone formation and resorption was shown to be associated with high risk of curve progression in AIS³⁵. Histomorphometry and fluorescent imaging studies suggested larger osteoid area, less osteocyte, aberrant structure and function of osteocyte lacuna-canalculi network in AIS bone tissues^{36,37}, which were partly attributed to differential expression profile of osteogenic genes in AIS osteoblasts^{38,39}. The molecular changes underlying these abnormalities could be a source of novel biomarkers.

Our recent study on bone tissues and patient-derived cell culture demonstrated a causative relationship between high miRNA-145-5p expression and abnormal osteocyte function in AIS⁴¹. In light of the close association between low bone mass and curve progression, we hypothesized that studying the miRNA profile in AIS bone tissues could lead to identification of novel miRNA candidates that are relevant to abnormal bone phenotypes in AIS. This study consisted of three parts: (1) we identified differentially expressed miRNAs by performing miRNA microarray on bone tissues collected from AIS and non-scoliotic subjects; (2) then, a retrospective case–control replication cohort was analyzed to determine the plasma levels of the selected miRNA candidates in AIS and healthy subjects; and (3) finally, logistic regression was applied to construct composite diagnostic models for AIS.

Results

Clinical and demographic characteristics of participants. Our initial discovery cohort was composed of four severe AIS patients and four age- and ethnically matched non-scoliotic subjects who underwent spinal fusion surgery and orthopaedic bone related reconstructive surgery, respectively. Both groups were recruited for collection of iliac crest bone tissues to identify miRNA candidates by miRNA microarray (Table 1 and Supplementary Table 1). This selection strategy for non-scoliotic subjects with low bone mass being the control group here was pivotal to distinguish miRNAs that were associated with AIS from those linked solely to low BMD. In validation cohort, one hundred AIS girls (with Cobb angles ranging from 15° to 80°) and fifty-two healthy girls were recruited. Anthropometric information, aBMD from DXA and bone quality parameters from HR-pQCT were summarized in Table 2. These two groups were similar to each other in terms of age, body height, arm span, sitting height, Tanner stage of pubic hair and year since menarche. AIS subjects were shown to have significantly lower body weight and slightly earlier Tanner breast stage. DXA results showed significantly lower aBMD at femoral necks in AIS girls than healthy girls. At distal radius, HR-pQCT analysis showed significantly lower cor-

	AIS girls (N = 100)	Healthy girls (N = 52)	P value
Age ^b	14.4 (13.6, 15.4)	14.8 (13.5, 15.8)	0.299
Maximum Cobb angle ^a	31.88 ± 13.55		
Anthropometric measurements			
Body weight (kg) ^a	43.7 ± 5.9	49.5 ± 10.3	< 0.001
Body height (cm) ^a	156.3 ± 5.7	156.2 ± 7	0.915
Arm span (cm) ^a	156.2 ± 6.8	154.1 ± 7.4	0.084
Sitting height (cm) ^b	84 (81.6, 85.5)	83.5 (80.9, 86.5)	0.750
Maturity assessment			
Tanner stage (breast) ^b	3 (3, 4)	4 (3, 4)	0.048
Tanner stage (pubic hair) ^b	3 (3, 4)	3 (3, 4)	0.552
Year since menarche ^a	2.3 ± 1.1	2.8 ± 1.8	0.083
DXA parameters			
Left femoral neck aBMD (g/cm ²) ^a	0.697 ± 0.067	0.827 ± 0.174	< 0.001
Right femoral neck aBMD (g/cm ²) ^a	0.706 ± 0.079	0.837 ± 0.18	< 0.001
HR-pQCT parameters			
Total area (mm ²) ^a	185.1 ± 32.6	180 ± 31.4	0.358
Cortical area (mm ²) ^b	37.7 (26.2, 46.2)	44.9 (30.2, 55.4)	0.007
Trabecular area (mm ²) ^a	143.6 ± 32.8	132.8 ± 30.9	0.051
Total vBMD (mg/HAm ³) ^b	279.9 (238.8, 329.5)	319.7 (253.1, 379.3)	0.004
Cortical vBMD (mg/HAm ³) ^b	763.3 (703.6, 828.7)	814.1 (741.1, 861.1)	0.014
Cortical thickness (mm) ^a	0.64 ± 0.26	0.78 ± 0.30	0.005
Cortical perimeter (mm) ^a	55.3 ± 5.0	54.7 ± 4.9	0.447
Trabecular vBMD (mg/HAm ³) ^a	136.2 ± 26.1	151.2 ± 35.9	0.009
Trabecular BV/TV ^a	0.113 ± 0.022	0.126 ± 0.03	0.009
Trabecular number (mm ⁻¹) ^a	1.575 ± 0.247	1.66 ± 0.281	0.056
Trabecular thickness (mm) ^b	0.072 (0.066, 0.077)	0.075 (0.065, 0.084)	0.148
Trabecular separation (mm) ^b	0.562 (0.508, 0.633)	0.526 (0.466, 0.598)	0.021

Table 2. Clinical and demographic characteristics of participants involved in validation cohort. ^aNormally distributed data were presented as mean ± standard deviation (SD) and independent samples t test was used. ^bData that were not normally distributed were presented as median (lower quartile, upper quartile). Mann–Whitney U test was used. Bold text indicated p value < 0.05

tical area, total vBMD, cortical vBMD, cortical thickness, trabecular vBMD, trabecular BV/TV and trabecular number with higher trabecular separation in AIS. These observations were comparable to previous studies³².

Differential miRNA profile in AIS bone tissues. A volcano plot (Fig. 1) was used to identify differentially expressed miRNAs in AIS bone. Thirty most differentially up- or down-regulated miRNAs in AIS bone tissues were summarized in Supplementary Table 2. Taken into consideration the fold change and statistical significance, miR-96-5p was selected due to its highest expression level among candidates with a 45.5-fold up-regulation when compared to non-scoliotic subjects. To get more insights into the mechanistic roles of our identified miRNAs in the molecular functions and their possible physiological roles in AIS pathogenesis, systematic gene pathway and network analyses were performed. Our analyses using the Ingenuity Pathway Analysis (IPA) software suggested that miR-96-5p targeting genes were playing more roles in abnormal morphology of bone and morphogenesis of skeletal system, and they were speculated to be associated with etiopathogenesis of scoliosis (Fig. 2).

Higher plasma level of miR-96-5p in AIS. The expressions of miR-96-5p in plasma of 100 patients with AIS and 52 healthy girls were compared. Plasma levels of miR-96-5p were found to be significantly higher in the AIS group ($p = 0.001$) (Fig. 3a). The power of Mann–Whitney U test in detecting the difference between AIS and healthy girls was estimated to be 0.85. Area under the curve (AUC) analysis demonstrated discriminating potency of plasma miR-96-5p between AIS and healthy girls, suggesting reasonably good diagnostic potential of miR-96-5p with AUC of 0.671 (95% CI, 0.579–0.763) shown in Fig. 3b.

Logistic regression models in distinguishing AIS patients from healthy controls. Logistic regression revealed that miR-96-5p along with body weight, femoral neck aBMD and total vBMD were significant predictors for the development of AIS (Table 3). The AUC for each variable was shown in Fig. 4. Given body weight, age and year since menarche are associated with curve progression and likely with onset of AIS^{42–44}, these variables were included in model 0 as the default model for further comparisons (Model 0 in Table 3 and AUC in Fig. 4h). Model 1 was composed of bone quality parameters and classical risk factors (body weight, age

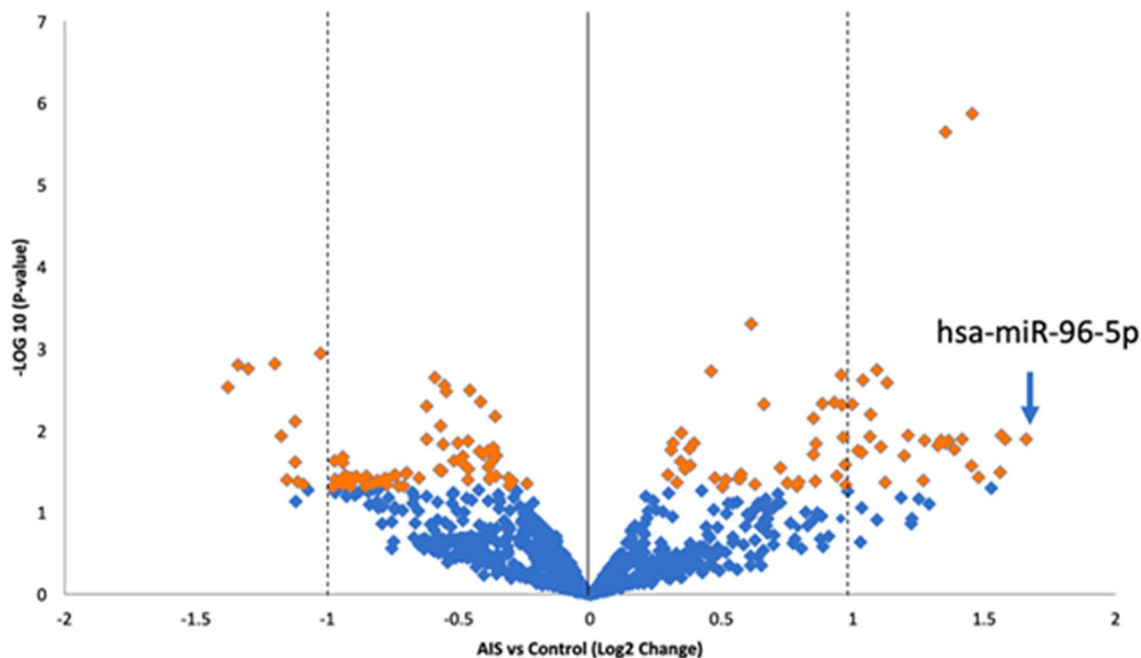


Figure 1. Differentially expressed miRNA candidates in iliac crest bone biopsies from AIS

and year since menarche) and explained 0.437 (Nagelkerke R^2) of the variances (Model 1 in Table 3 and AUC in Fig. 4i). Model 2 containing miR-96-5p and variables in Model 1 showed the highest Nagelkerke R^2 of 0.461 (Model 2 in Table 3) with AUC being 0.817 (95% CI 0.722–0.912, Fig. 4j). The addition of miR-96-5p increased the Nagelkerke R^2 of Model 0 with classical risk factors from 20.9% to 27.5% in Model 3 (Table 3). Meanwhile, the inclusion of miR-96-5p increased the AUC from 0.721 (95% CI 0.622–0.820) in Model 0 to 0.752 (95% CI 0.660–0.844) in Model 3 (Fig. 4k). The variable importance in each model was shown in Fig. 5.

Discussion

Significantly, higher expression levels of the miR-96-5p in AIS were shown in plasma samples from a retrospective case–control cohort. After excluding irrelevant or redundancy information that was leading to overfitting, a composite model composed of plasma miR-96-5p level, age, years since menarche and body weight was established and showed to have an AUC of 0.752 (95% CI 0.660–0.844) without bone qualities scan by DXA and HR-pQCT, indicating its potential to serve as clinically useful minimal invasive diagnostic biomarker for AIS.

The pathomechanism underlying the abnormal bone qualities has been one of the major research areas to understand the pathogenesis of AIS¹. The findings of current genetic studies are far from reaching a consensus on biological contribution of individual single nucleotide polymorphisms (SNPs) to AIS pathogenesis. It appears that either single or multiple SNPs can only explain onset of AIS in small proportion of patients^{45,46}. In view that AIS is a complex disease, the potential of epigenetics to explain its complexity and clinical heterogeneity represents a largely unexplored research field. Previous studies which relied on whole blood cells for the identification of prognostic biomarker candidates for AIS showed limited success^{28,47}. Furthermore, given that DNA methylation patterns are often tissue specific, investigations focusing on DNA methylation alterations in whole blood cell of AIS patients are unlikely to be successful to decipher AIS pathogenesis^{48–50}. Indeed, a large cohort study on 5515 individuals indicated a lack of association between epigenetic changes in whole blood and bone mineral density⁵¹. Therefore, we developed a more direct approach by investigating bone tissues in our discovery phase to identify miRNA candidates, which were likely to be more biologically relevant to the abnormal bone qualities in AIS.

Emerging evidence suggested that aberrant expression of several non-coding RNAs in AIS impaired cellular activities of mesenchymal stromal cells and osteoblasts/osteocytes^{41,52,53}, which may account for the observed phenotypic changes affecting bone metabolism and bone qualities in AIS. In contrast to lncRNA, the stability of miRNA in biofluids renders its superiority for being biomarkers to reflect molecular alterations in complex diseases such as AIS^{54,55}. The miR-96-5p identified in the present study had controversial effects on osteogenic activity. Yang et al. reported that miR-96 promoted the osteogenic ability of murine osteoblasts and bone marrow-derived mesenchymal stem cells⁵⁶, and inhibits the proliferation of vascular smooth muscle cells⁵⁷. Another publication showed that higher levels of miR-96 were associated with age-related bone loss⁵⁸. Intravenous injection of agomiR-96 to 3-month-old mice induced defective osteogenesis by targeting osterix gene and the mice manifested low bone mass⁵⁸. This in vivo evidence was supportive of observation in our current study that overexpression of miR-96-5p was associated with low bone mass and AIS in young Chinese adolescents. Our group previously reported that miR-145-5p impaired osteocytes activities and differentiation in AIS⁴¹ and it was a significant factor in a predictive model to predict whether the curve progressed to a Cobb angle of 40°⁵⁹.

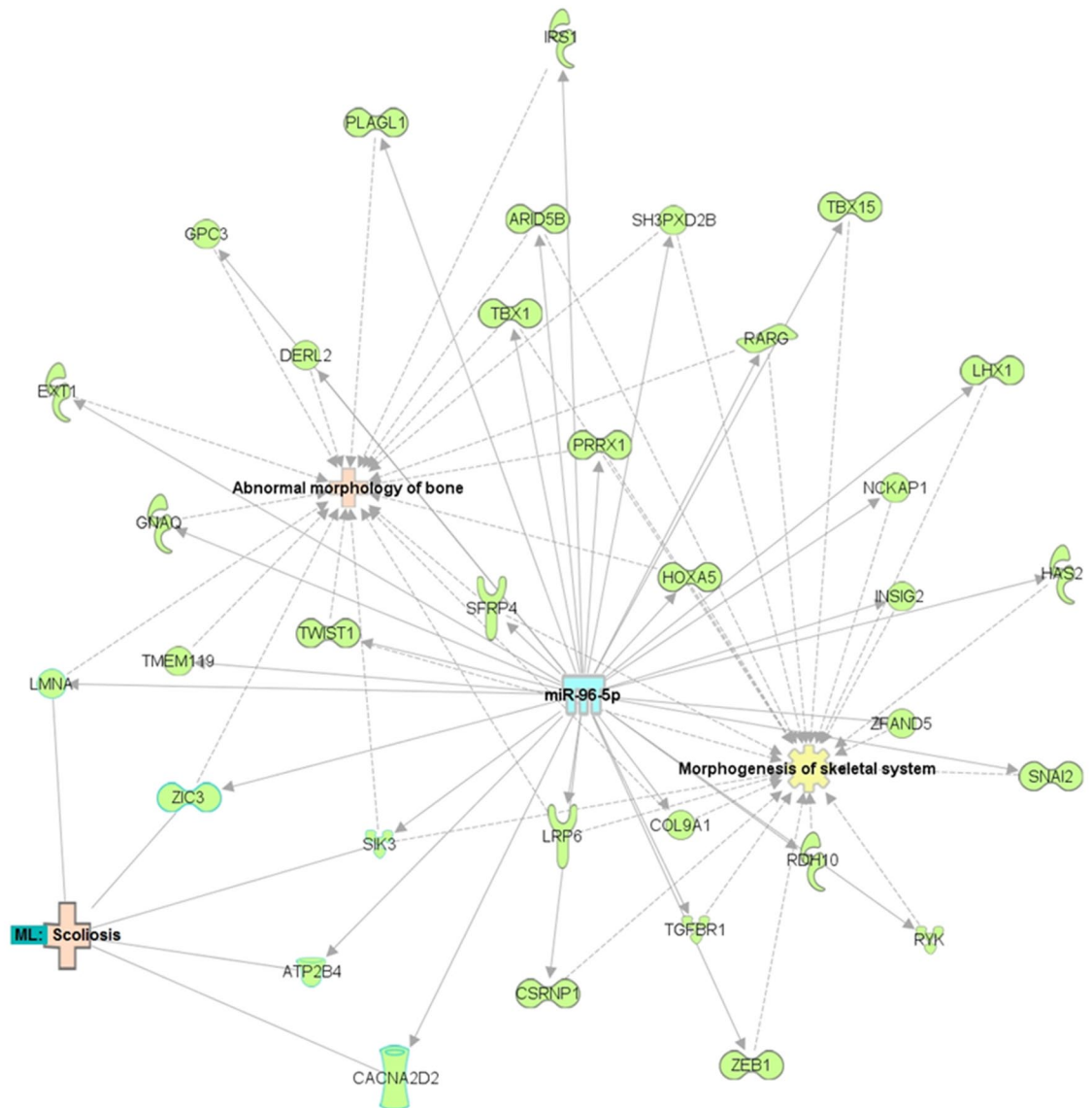


Figure 2. Predicted gene pathways and network of miR-96-5p. The miRNA is represented in blue; the genes that were predicted to interact with each other are in green; the diseases that were predicted to be associated with the miRNA or genes are in light pink; and the molecular and physiological functions are in yellow. The hybrid approach of IPA and manual curations was applied to construct the network of miR-96-5p.

Although the miRNA candidates were identified in bone tissues, it was of interest to provide functional evidence about their known and predicted downstream targets as well as their putative role in bone homeostasis.

There are several limitations of our current study. First, our validation cohort was cross-sectional by design. Our participants were skeletally immature, and we did not follow them until their skeletal maturity to determine the predictive potential of our miRNAs and models in prediction of the risk of spinal disease progression among a symptomatic population at an early stage. Therefore, a new prospective study with long-term follow-up is warranted. Secondly, expression of miR-96-5p was reported to be regulated by oestrogens (E2), implying the likelihood of a sexual dimorphism on this regard⁶⁰. Indeed, one could reasonably speculate that the elevation of miR-96-5p was influenced by the hormonal rise, which could explain why girls are more predisposed to curve progression around puberty than boys. The present study only validated the abnormal expression of miR-96-5p in girls and future validations in both females and males are required to clarify whether expression of miR-96-5p is abnormal in male AIS patients and whether it is different between genders. Third, although abnormal miRNAs that were identified in bone tissue in AIS have been validated in our previous work (miR-145-5p) and the present study (miR-96-5p), a combination of multiple biomarkers from different omics layers is warranted in future work to achieve an optimal effectiveness in early detection or prognostication for AIS.

In summary, this study proposed a predictive model for AIS using pathology-associated clinical features such as low bone mass and aetiology-associated circulating miR-96-5p levels, which possessed the ability to distinguish AIS patients from healthy controls. This study addressed the outstanding clinical question for a reliable diagnosis

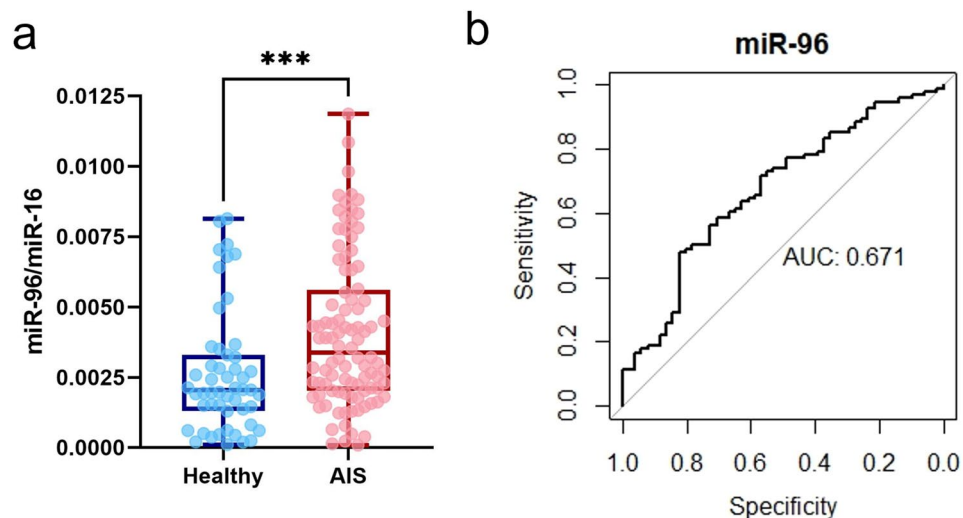


Figure 3. Plasma miR-96-5p levels in AIS and healthy girls. **(a)** Difference of plasma levels of miR-96-5p between AIS and healthy girls. Expression levels of miR-96-5p was normalized by plasma miR-16 levels. *** $p \leq 0.001$. **(b)** Receiver operating characteristic (ROC) curve and AUC of plasma miR-96-5p level.

system of AIS at the early presentation of AIS, which has important clinical implications for clinical decisions to prevent onset and to avoid over-treatment and frequent radio-exposure.

Methodology

Study populations. Patients undergoing surgery were recruited for microarray assay. Trabecular bone tissues were intraoperatively collected from iliac crests of AIS patients who underwent spinal fusion surgery as a part of taking autograft to enhance bony fusion. Trabecular bone tissues from non-scoliotic controls were collected from trauma cases who needed iliac crest bone tissues during orthopedics surgery. To investigate the clinical implication of circulating miRNAs, patients were recruited in a case-control cohort. Anthropometrical parameters including standing height, sitting height, body weight and arm span were measured with standard protocols. AIS was diagnosed clinically by at least two senior orthopedic surgeons and radiologically with standing full-spine posteroanterior (PA) X-ray. HR-pQCT measurement, DXA measurement and full-spine PA X-ray for Cobb angle of the major curve were performed within a month before or after the date when blood samples were taken. In the case-control cohort, one hundred AIS girls were recruited from the scoliosis clinic in Prince of Wales Hospital, Hong Kong. Fifty-two aged matched healthy girls were recruited randomly from local secondary school as control. Exclusion criteria included subjects with congenital deformities, neuromuscular diseases, autoimmune disorders, endocrine disturbances or other medical conditions that affecting bone metabolism. Ethical approval in accordance with Declaration of Helsinki was obtained from Clinical Research Ethics Committee of the University and Hospital (CREC No. 2016.567). Written informed consent was obtained from all the subjects and their legal guardians before the examinations and measurements.

BMD and bone qualities assessment. aBMD of bilateral femoral necks was measured by DXA (XR-46; Norland Medical Systems, Wisconsin, USA). Due to the bias caused by axial vertebral rotation in AIS, aBMD of the spine measured by DXA should not be used in AIS⁶¹. The detail of DXA measurement was presented in our previous study³². The 3-dimensional assessment of bone qualities in the non-dominant distal radius was measured with HR-pQCT (XtremeCT I, Scanco Medical, Brüttisellen, Switzerland) according to the standard protocols⁶². Reference line was marked at the most proximal point of the inner aspect of the growth plate. One-hundred-ten computed tomography slices with a resolution of 82 μm were obtained from a segment spanning 9.02 mm starting from 5 mm proximal to the reference line.

miRNA microarray on bone biopsies. Total RNA was extracted from iliac crest bone biopsies from 4 AIS and 4 non-scoliotic subjects with TRIZOL (Life technologies, California, USA) based on manufacturer's instruction. RNA integrity was tested with Agilent Bioanalyzer 2100 (Agilent Technologies, Palo Alto, California, USA) to ensure satisfactory RNA integrity and quality before microarray assay. Differentially expressed miRNAs were identified by Agilent expression array-Human miRNA 8 \times 60k (Agilent Technologies, Palo Alto, CA, USA) with 100 ng of total RNA. Agilent microarray could identify all mature miRNA sequences in the latest miRBase (version 21.0) with high sensitivity and wide coverage. Data processing was conducted with GeneSpring station (version 12.6).

Construction of gene pathways and networks targeted by dysregulated miRNAs in AIS. The potential targets of miRNAs of interest, including genes, molecular and physiological functions in AIS patho-

	β	Standard error	Z value	P value	95% CI for β	
					Lower limit	Upper limit
Model 0						
Age	-0.028	0.226	-0.126	0.899	-0.478	0.415
Year since menarche	-0.059	0.187	-0.316	0.751	-0.430	0.310
Body weight	-0.120	0.032	-3.657	<0.001	-0.190	-0.060
Constant	6.910	3.50	1.969	0.048		
Nagelkerke R-squared	0.209					
Model 1						
Age	0.234	0.262	0.890	0.371	-0.276	0.762
Year since menarche	0.195	0.239	0.820	0.415	-0.266	0.682
Body weight	-0.064	0.042	-1.540	0.124	-0.150	0.013
Left femoral neck aBMD	-10.500	3.040	-3.460	<0.001	-16.934	-4.944
Total vBMD	-0.007	0.004	-1.580	0.114	-0.015	0.001
Trabecular vBMD	1.160	0.729	1.580	0.113	-0.252	0.262
Trabecular BV/TV	-1380.000	877.000	-1.580	0.114	-3155.600	308.790
Constant	96.10	4.100	2.350	0.019		
Nagelkerke R-squared	0.437					
Model 2						
ln (miR-96)	0.504	0.255	1.975	0.048	0.013	1.028
Age	0.234	0.269	0.871	0.383	-0.287	0.776
Year since menarche	0.337	0.250	1.345	0.178	-0.142	0.852
Body weight	-0.078	0.042	-1.854	0.063	-0.166	0.0001
Left femoral neck aBMD	-9.343	3.108	-3.006	0.0026	-15.907	-3.652
Total vBMD	-0.009	0.005	-1.925	0.054	-1.852	6.134
Trabecular vBMD	1.200	0.744	1.613	0.106	-0.235	2.704
Trabecular BV/TV	-1431.000	894.800	-1.599	0.109	-3238.296	296.308
Constant	11.900	4.341	2.740	0.006		
Nagelkerke R-squared	0.461					
Model 3						
ln (miR-96)	0.607	0.221	2.737	0.006	0.190	1.07
Age	-0.044	0.237	-0.189	0.850	-0.516	0.421
Year since menarche	0.071	0.193	0.367	0.713	-0.310	0.456
Body weight	-0.127	0.033	-3.853	<0.001	-0.197	-0.067
Constant	10.850	3.988	2.721	0.006		
Nagelkerke R-squared	0.275					

Table 3. Logistic regression models to predict AIS. Plasma level of miR-96-5p with log transformation, maximum Cobb angle at first visit, maturity (age, years since menarche), anthropometry (body weight, body height), left femoral neck aBMD, and bone qualities at distal radius (total area, cortical area, trabecular area, total vBMD, cortical vBMD, cortical thickness, cortical perimeter, trabecular vBMD, BV/TV, trabecular number, trabecular thickness, trabecular separation) were put into backward stepwise regression to select the important parameters for model 2. Bold text indicated p value < 0.05.

genesis were primarily identified through a comprehensive literature review and manual curations. The connections (interactions) of the miRNAs and their targets were constructed based on the Ingenuity Knowledge Base using the Ingenuity Pathway Analysis (IPA) software (QIAGEN Inc. software version 51,963,813).

Plasma miRNA level assay. Peripheral venous blood samples from subjects were collected by phlebotomists with standard technique. Blood was centrifuged at 4 °C and 1500×g for 10 min. Plasma was aliquoted and stored at -80 °C for further analysis. Thaw-freeze cycle was avoided in case of degradation. Isolation of circulating miRNAs from plasma was performed with miRNeasy plasma advanced kit (217204, Qiagen, Venlo, The Netherlands) according to manufacturer's protocol. cDNA library was constructed, and target miRNA expression levels were measured with TaqMan® advanced miRNA assay (Life Technologies, California, USA). miR-16 was chosen as an internal reference after evaluating its stability in BestKeeper (<http://www.gene-quantification.de/bestkeeper.html/>).

Statistical analysis. The normality of data was tested by Shapiro–Wilk test. Normal data was presented as mean ± SD and the other was presented as median (lower quartile, upper quartile). To compare the parameters between AIS and non-scoliotic controls, independent sample t test was used for the normal data, and the Mann–

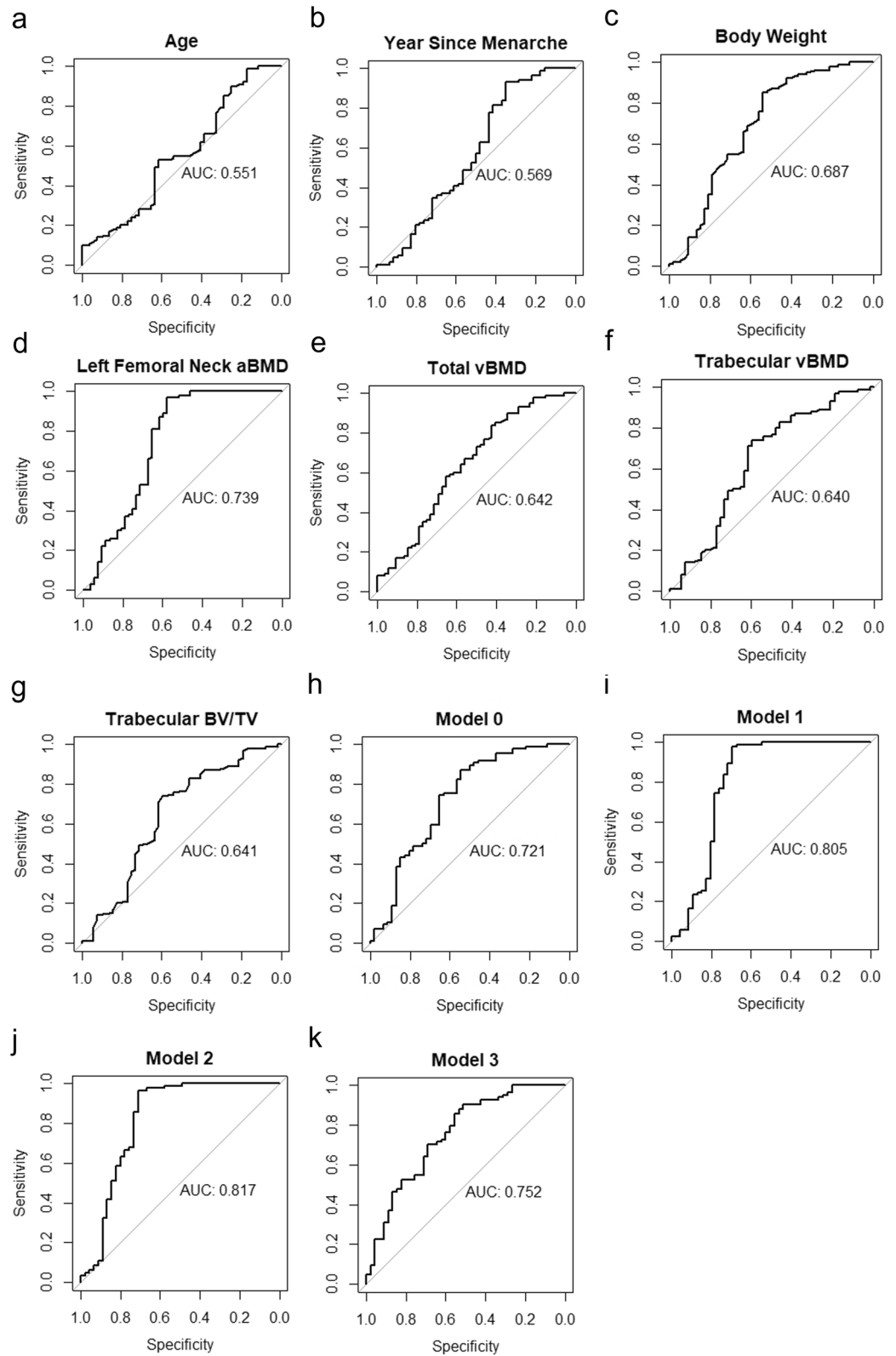


Figure 4. ROC curves and AUC of variables and logistic regression models.

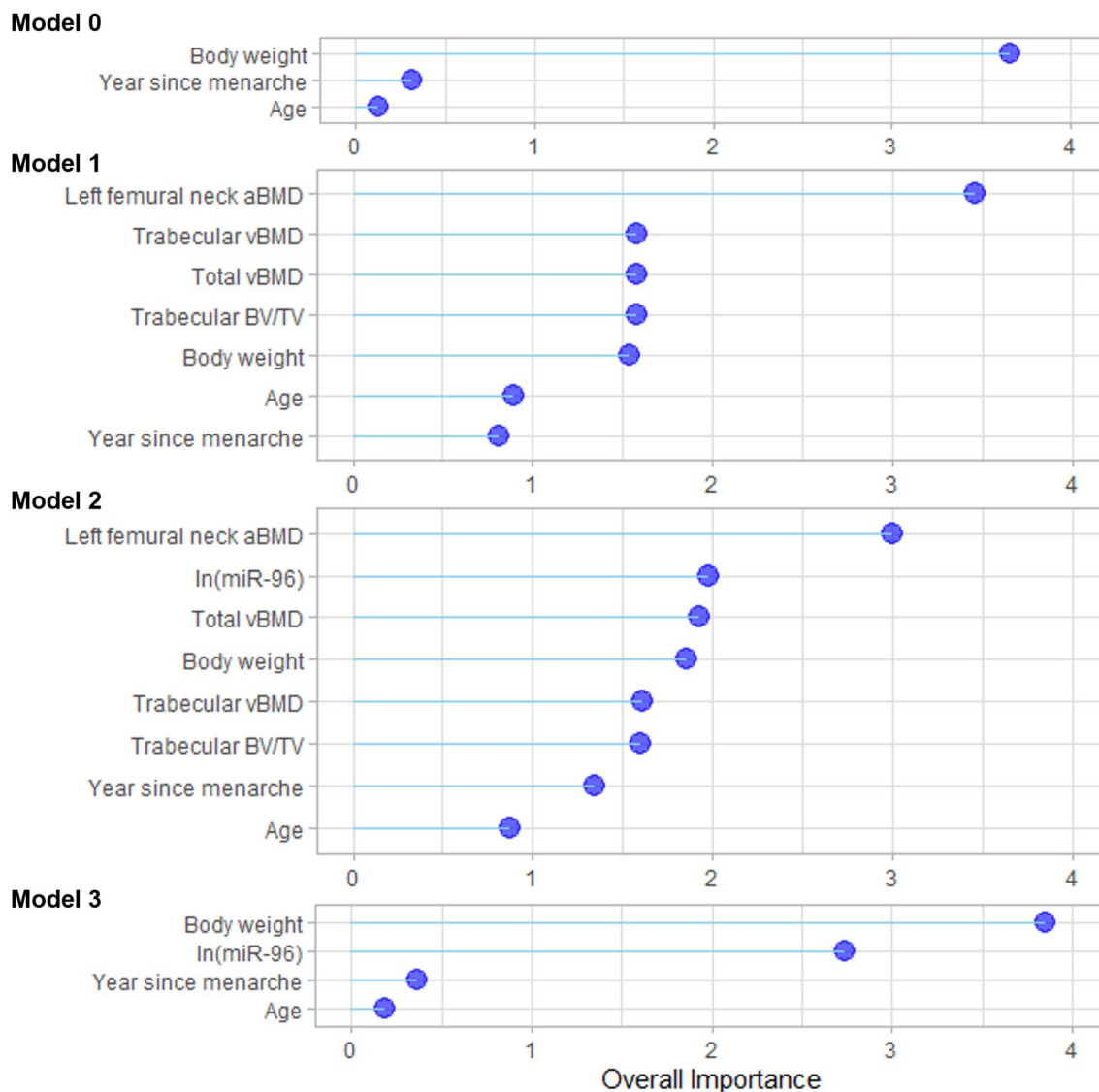


Figure 5. Variable importance in logistic regression models.

Whitney U test was used for the skewed data. Analysis of covariance (ANCOVA) analysis was used to compare miRNA levels between AIS and healthy girls with adjustment to age. Backward stepwise regression was used to determine whether the plasma miRNA is an important predictor in classifying AIS from non-scoliotic subjects with adjustment for bone maturity, body size, bone qualities by HR-pQCT and aBMD by DXA. In the logistic regression, plasma miRNA levels were transformed with natural log transformation. The factor was dichotomised with criteria shown as follows: 1 as logistic score ≥ 0.5 and 0 as logistic score < 0.5 . ROC curves and the binary classification tables were used to study sensitivity and specificity. Variable importance was estimated using a method described by Gevery et al.⁶³ P-values < 0.05 (two-tailed) indicated statistical significance. Data collection and analyses were performed by two blinded investigators independently. Analyses were performed using R (version 4.0.0, The R Foundation, Vienna, Austria). Effect size of AIS status on expression of miR-96-5p was calculated by dividing the difference between means pertaining to AIS and healthy girls by SD of the whole validation cohort. Power of statistical testing were estimated by G*Power (version 3.1.9.6, Kiel University, Germany) with α being 0.05.

Ethics declarations. Ethical approval in accordance with Declaration of Helsinki was obtained from Clinical Research Ethics Committee of the University and Hospital (CREC No. 2016.567). Written informed consent was obtained from all the subjects and their legal guardians before the examinations and measurements.

Data availability

The data that support the findings of this study are available from the corresponding author upon reasonable request.

Received: 8 December 2021; Accepted: 18 May 2022

Published online: 11 June 2022

References

- Cheng, J. C. *et al.* Adolescent idiopathic scoliosis. *Nat. Rev. Dis. Primers* **1**, 15030. <https://doi.org/10.1038/nrdp.2015.30> (2015).
- Weinstein, S. L., Dolan, L. A., Cheng, J. C., Danielsson, A. & Morcuende, J. A. Adolescent idiopathic scoliosis. *Lancet* **371**, 1527–1537. [https://doi.org/10.1016/S0140-6736\(08\)60658-3](https://doi.org/10.1016/S0140-6736(08)60658-3) (2008).
- van Rhijn, L. W., Jansen, E. J., Plasmans, C. M. & Veraart, B. E. Curve characteristics in monozygotic twins with adolescent idiopathic scoliosis: 3 new twin pairs and a review of the literature. *Acta Orthop. Scand.* **72**, 621–625. <https://doi.org/10.1080/000164701317269058> (2001).
- Zaydman, A. M. *et al.* Etiopathogenesis of adolescent idiopathic scoliosis: Review of the literature and new epigenetic hypothesis on altered neural crest cells migration in early embryogenesis as the key event. *Med. Hypotheses* **151**, 110585. <https://doi.org/10.1016/j.mehy.2021.110585> (2021).
- Xu, L. L. *et al.* A functional SNP in the promoter of LBX1 is associated with the development of adolescent idiopathic scoliosis through involvement in the myogenesis of paraspinal muscles. *Front. Cell Dev. Biol.* <https://doi.org/10.3389/fcell.2021.777890> (2021).
- Wang, Y. *et al.* Role of differentially expressed LBX1 in Adolescent Idiopathic Scoliosis (AIS) paraspinal muscle phenotypes and muscle-bone crosstalk through modulating myoblasts. *Stud. Health Technol. Inform.* **280**, 14–17. <https://doi.org/10.3233/SHTI210425> (2021).
- Fan, Y. H. *et al.* SNP rs11190870 near LBX1 is associated with adolescent idiopathic scoliosis in southern Chinese. *J. Hum. Genet.* **57**, 244–246. <https://doi.org/10.1038/jhg.2012.11> (2012).
- Londono, D. *et al.* A meta-analysis identifies adolescent idiopathic scoliosis association with LBX1 locus in multiple ethnic groups. *J. Med. Genet.* **51**, 401–406. <https://doi.org/10.1136/jmedgenet-2013-102067> (2014).
- Pérez-Machado, G. *et al.* From genetics to epigenetics to unravel the etiology of adolescent idiopathic scoliosis. *Bone* **140**, 115563. <https://doi.org/10.1016/j.bone.2020.115563> (2020).
- Moore, L. D., Le, T. & Fan, G. DNA methylation and its basic function. *Neuropsychopharmacology* **38**, 23–38. <https://doi.org/10.1038/npp.2012.112> (2013).
- Carry, P. M. *et al.* Severity of idiopathic scoliosis is associated with differential methylation: An epigenome-wide association study of monozygotic twins with idiopathic scoliosis. *Genes-Basel.* <https://doi.org/10.3390/genes12081191> (2021).
- Janusz, P., Chmielewska, M., Andrusiewicz, M., Kotwicka, M. & Kotwicki, T. Methylation of estrogen receptor 1 gene in the paraspinal muscles of girls with idiopathic scoliosis and its association with disease severity. *Genes (Basel)* <https://doi.org/10.3390/genes12060790> (2021).
- Chmielewska, M., Janusz, P., Andrusiewicz, M., Kotwicki, T. & Kotwicki, M. Methylation of estrogen receptor 2 (ESR2) in deep paravertebral muscles and its association with idiopathic scoliosis. *Sci. Rep.* **10**, 22331. <https://doi.org/10.1038/s41598-020-78454-4> (2020).
- Shi, B. *et al.* Quantitation analysis of PCDH10 methylation in adolescent idiopathic scoliosis using pyrosequencing study. *Spine (Phila Pa 1976)* **45**, E373–E378. <https://doi.org/10.1097/BRS.0000000000003292> (2020).
- Chidambaram, V. *et al.* DNA methylation at the mu-1 opioid receptor gene (OPRM1) promoter predicts preoperative, acute, and chronic postsurgical pain after spine fusion. *Pharmacogen. Pers. Med.* **10**, 157–168. <https://doi.org/10.2147/Pgpm.S132691> (2017).
- Ogura, Y., Matsumoto, M., Ikegawa, S. & Watanabe, K. Epigenetics for curve progression of adolescent idiopathic scoliosis. *EBio-Medicine* **37**, 36–37. <https://doi.org/10.1016/j.ebiom.2018.10.015> (2018).
- Shi, B. *et al.* Abnormal PITX1 gene methylation in adolescent idiopathic scoliosis: A pilot study. *BMC Musculoskelet. Disord.* **19**, 138. <https://doi.org/10.1186/s12891-018-2054-2> (2018).
- Li, J. *et al.* Suv39h1 promotes facet joint chondrocyte proliferation by targeting miR-15a/Bcl2 in idiopathic scoliosis patients. *Clin. Epigenet.* **11**, 107. <https://doi.org/10.1186/s13148-019-0706-1> (2019).
- Liu, G. *et al.* Whole-genome methylation analysis of phenotype discordant monozygotic twins reveals novel epigenetic perturbation contributing to the pathogenesis of adolescent idiopathic scoliosis. *Front. Bioeng. Biotech.* <https://doi.org/10.3389/fbioe.2019.00364> (2019).
- Statello, L., Guo, C. J., Chen, L. L. & Huarte, M. Gene regulation by long non-coding RNAs and its biological functions. *Nat. Rev. Mol. Cell Biol.* **22**, 96–118. <https://doi.org/10.1038/s41580-020-00315-9> (2021).
- Jiang, H. *et al.* Asymmetric expression of H19 and ADIPOQ in concave/convex paravertebral muscles is associated with severe adolescent idiopathic scoliosis. *Mol. Med.* **24**, 48. <https://doi.org/10.1186/s10020-018-0049-y> (2018).
- Liu, X. Y., Wang, L., Yu, B., Zhuang, Q. Y. & Wang, Y. P. Expression signatures of long noncoding RNAs in adolescent idiopathic scoliosis. *Biomed. Res. Int.* <https://doi.org/10.1155/2015/276049> (2015).
- Yu, M. *et al.* Signal inhibition by the dual-specific phosphatase 4 impairs T cell-dependent B-cell responses with age. *Proc. Natl. Acad. Sci. U S A* **109**, E879–888. <https://doi.org/10.1073/pnas.1109797109> (2012).
- Yang, Q., Qiu, C., Yang, J., Wu, Q. & Cui, Q. miREnvironment database: Providing a bridge for microRNAs, environmental factors and phenotypes. *Bioinformatics* **27**, 3329–3330. <https://doi.org/10.1093/bioinformatics/btr556> (2011).
- Weber, J. A. *et al.* The microRNA spectrum in 12 body fluids. *Clin. Chem.* **56**, 1733–1741. <https://doi.org/10.1373/clinchem.2010.147405> (2010).
- Wang, Y. J. *et al.* Dysregulated bone metabolism is related to high expression of miR-151a-3p in severe adolescent idiopathic scoliosis. *Biomed. Res. Int.* <https://doi.org/10.1155/2020/4243015> (2020).
- Huang, F. L. *et al.* Incidence of scoliosis among junior high school students in Zhongshan city, Guangdong and the possible importance of decreased miR-30e expression. *J. Int. Med. Res.* <https://doi.org/10.1177/0300060519889438> (2020).
- García-Giménez, J. L. *et al.* Circulating miRNAs as diagnostic biomarkers for adolescent idiopathic scoliosis. *Sci. Rep.* **8**, 2646. <https://doi.org/10.1038/s41598-018-21146-x> (2018).
- Hung, V. W. *et al.* Osteopenia: A new prognostic factor of curve progression in adolescent idiopathic scoliosis. *J. Bone Joint Surg. Am.* **87**, 2709–2716. <https://doi.org/10.2106/JBJS.D.02782> (2005).
- Cheng, J. C., Guo, X. & Sher, A. H. Persistent osteopenia in adolescent idiopathic scoliosis. A longitudinal follow up study. *Spine (Phila Pa 1976)* **24**, 1218–1222. <https://doi.org/10.1097/00007632-199906150-00008> (1999).
- Cheung, C. S. *et al.* Generalized osteopenia in adolescent idiopathic scoliosis—Association with abnormal pubertal growth, bone turnover, and calcium intake?. *Spine* **31**, 330–338. <https://doi.org/10.1097/01.brs.0000197410.92525.10> (2006).
- Cheuk, K. Y. *et al.* Abnormal bone mechanical and structural properties in adolescent idiopathic scoliosis: A study with finite element analysis and structural model index. *Calcif. Tissue Int.* **97**, 343–352. <https://doi.org/10.1007/s00223-015-0025-2> (2015).
- Wang, Z. W. *et al.* Defining the bone morphometry, micro-architecture and volumetric density profile in osteopenic vs non-osteopenic adolescent idiopathic scoliosis. *Eur. Spine J.* **26**, 1586–1594. <https://doi.org/10.1007/s00586-016-4422-7> (2017).
- Yip, B. H. *et al.* Prognostic value of bone mineral density on curve progression: A longitudinal cohort study of 513 girls with adolescent idiopathic scoliosis. *Sci. Rep.* **6**, 39220. <https://doi.org/10.1038/srep39220> (2016).
- Zhang, J. *et al.* Association of higher bone turnover with risk of curve progression in adolescent idiopathic scoliosis. *Bone* **143**, 115655. <https://doi.org/10.1016/j.bone.2020.115655> (2021).

36. Chen, H. *et al.* Abnormal lacuno-canalicular network and negative correlation between serum osteocalcin and Cobb angle indicate abnormal osteocyte function in adolescent idiopathic scoliosis. *FASEB J.* **33**, 13882–13892. <https://doi.org/10.1096/fj.201901227R> (2019).
37. Wang, Z. *et al.* Unique local bone tissue characteristics in iliac crest bone biopsy from adolescent idiopathic scoliosis with severe spinal deformity. *Sci. Rep.* **7**, 40265. <https://doi.org/10.1038/srep40265> (2017).
38. Man, G. C. *et al.* Abnormal melatonin receptor 1B expression in osteoblasts from girls with adolescent idiopathic scoliosis. *J. Pineal Res.* **50**, 395–402. <https://doi.org/10.1111/j.1600-079X.2011.00857.x> (2011).
39. Fendri, K. *et al.* Microarray expression profiling identifies genes with altered expression in adolescent idiopathic scoliosis. *Eur Spine J.* **22**, 1300–1311. <https://doi.org/10.1007/s00586-013-2728-2> (2013).
40. Garcia-Gimenez, J. L. *et al.* Circulating miRNAs as diagnostic biomarkers for adolescent idiopathic scoliosis. *Sci. Rep.* <https://doi.org/10.1038/s41598-018-21146-x> (2018).
41. Zhang, J. *et al.* Aberrant miR-145-5p/beta-catenin signal impairs osteocyte function in adolescent idiopathic scoliosis. *FASEB J.* <https://doi.org/10.1096/fj.201800281> (2018).
42. Cheung, C. S. K. *et al.* Abnormal peri-pubertal anthropometric measurements and growth pattern in adolescent idiopathic scoliosis: A study of 598 patients. *Spine (Phila Pa 1976)* **28**, 2152–2157. <https://doi.org/10.1097/01.BRS.0000084265.15201.D5> (2003).
43. Ylikoski, M. Growth and progression of adolescent idiopathic scoliosis in girls. *J Pediatr Orthop B* **14**, 320–324. <https://doi.org/10.1097/01202412-200509000-00002> (2005).
44. Lenz, M. *et al.* Scoliosis and prognosis—A systematic review regarding patient-specific and radiological predictive factors for curve progression. *Eur. Spine J.* **30**, 1813–1822. <https://doi.org/10.1007/s00586-021-06817-0> (2021).
45. Zhu, Z. *et al.* Genome-wide association study identifies new susceptibility loci for adolescent idiopathic scoliosis in Chinese girls. *Nat. Commun.* **6**, 8355. <https://doi.org/10.1038/ncomms9355> (2015).
46. Ogura, Y. *et al.* A replication study for association of 53 single nucleotide polymorphisms in a scoliosis prognostic test with progression of adolescent idiopathic scoliosis in Japanese. *Spine (Phila Pa 1976)* **38**, 1375–1379. <https://doi.org/10.1097/BRS.0b013e3182947d21> (2013).
47. Meng, Y. *et al.* Value of DNA methylation in predicting curve progression in patients with adolescent idiopathic scoliosis. *EBio-Medicine* **36**, 489–496. <https://doi.org/10.1016/j.ebiom.2018.09.014> (2018).
48. Houseman, E. A., Kim, S., Kelsey, K. T. & Wiencke, J. K. DNA methylation in whole blood: Uses and challenges. *Curr. Environ. Health Rep.* **2**, 145–154. <https://doi.org/10.1007/s40572-015-0050-3> (2015).
49. Hawkins, R. D. *et al.* Distinct epigenomic landscapes of pluripotent and lineage-committed human cells. *Cell Stem Cell* **6**, 479–491. <https://doi.org/10.1016/j.stem.2010.03.018> (2010).
50. Lister, R. *et al.* Human DNA methylomes at base resolution show widespread epigenomic differences. *Nature* **462**, 315–322. <https://doi.org/10.1038/nature08514> (2009).
51. Morris, J. A. *et al.* Epigenome-wide association of DNA methylation in whole blood with bone mineral density. *J. Bone Miner. Res.* **32**, 1644–1650. <https://doi.org/10.1002/jbmr.3148> (2017).
52. Zhuang, Q. *et al.* Long noncoding RNA lncAIS downregulation in mesenchymal stem cells is implicated in the pathogenesis of adolescent idiopathic scoliosis. *Cell Death Differ.* <https://doi.org/10.1038/s41418-018-0240-2> (2018).
53. Hui, S. *et al.* Differential miRNAs profile and bioinformatics analyses in bone marrow mesenchymal stem cells from adolescent idiopathic scoliosis patients. *Spine J.* **19**, 1584–1596. <https://doi.org/10.1016/j.spinee.2019.05.003> (2019).
54. Seeliger, C. *et al.* Five freely circulating miRNAs and bone tissue miRNAs are associated with osteoporotic fractures. *J. Bone Miner. Res.* **29**, 1718–1728. <https://doi.org/10.1002/jbmr.2175> (2014).
55. Heilmeyer, U. *et al.* Serum miRNA signatures are indicative of skeletal fractures in postmenopausal women with and without type 2 diabetes and influence osteogenic and adipogenic differentiation of adipose tissue-derived mesenchymal stem cells in vitro. *J. Bone Miner. Res.* **31**, 2173–2192. <https://doi.org/10.1002/jbmr.2897> (2016).
56. Yang, M., Pan, Y. & Zhou, Y. miR-96 promotes osteogenic differentiation by suppressing HBEGF–EGFR signaling in osteoblastic cells. *FEBS Lett.* **588**, 4761–4768. <https://doi.org/10.1016/j.febslet.2014.11.008> (2014).
57. Wallace, E. *et al.* A sex-specific microRNA-96/5-hydroxytryptamine 1B axis influences development of pulmonary hypertension. *Am. J. Respir. Crit. Care Med.* **191**, 1432–1442. <https://doi.org/10.1164/rccm.201412-2148OC> (2015).
58. Liu, H., Liu, Q., Wu, X. P., He, H. B. & Fu, L. MiR-96 regulates bone metabolism by targeting osterix. *Clin. Exp. Pharmacol. Physiol.* **45**, 602–613. <https://doi.org/10.1111/1440-1681.12912> (2018).
59. Zhang, J. *et al.* A validated composite model to predict risk of curve progression in adolescent idiopathic scoliosis. *EClinicalMedicine* **18**, 100236. <https://doi.org/10.1016/j.eclinm.2019.12.006> (2020).
60. Morgan, C. P. & Bale, T. L. Sex differences in microRNA-mRNA networks: Examination of novel epigenetic programming mechanisms in the sexually dimorphic neonatal hypothalamus. *Biol. Sex Differ.* **8**, 27. <https://doi.org/10.1186/s13293-017-0149-3> (2017).
61. Cheng, J. C., Sher, H. L., Guo, X., Hung, V. W., & Cheung, A. Y. The effect of vertebral rotation of the lumbar spine on dual energy X-ray absorptiometry measurements: Observational study. *Hong Kong Med J.* **7**, 241–245 (2001)
62. Kirmani, S. *et al.* Bone structure at the distal radius during adolescent growth. *J. Bone Miner. Res.* **24**, 1033–1042. <https://doi.org/10.1359/jbmr.081255> (2009).
63. Gevrey, M. Review and comparison of methods to study the contribution of variables in artificial neural network models. *Ecological Modelling*, **160**, 249–264. [https://doi.org/10.1016/S0304-3800\(02\)00257-0](https://doi.org/10.1016/S0304-3800(02)00257-0) (2003).

Acknowledgements

This work was partially supported by National Natural Science Foundation of China (81902270 and 82160435 to HX Chen), Young Talents' Science and Technology Innovation Project of Hainan Association for Science and Technology (QCXM202014) and Hainan Province Clinical Medical Center, the research funding by The Cotrel Foundation at Institut de France (to A Moreau), the Research Grants Council of the Hong Kong S.A.R., China (Project 14120818 to WYW Lee), and the Health and Medical Research Fund (06170546 to WYW Lee).

Author contributions

A.M., W.L. and H.C. conceived the study and design; J.Z., K.C. and K.Y. performed experiments and data analysis; Y. W. assisted in serological sample collection; J. Z., K.Y., W. L. and H.C. drafted the manuscript; H.C., T.L. and A.H. assisted in samples collection and clinical data acquisition; E.N. performed IPA analysis; W.L. and A.M. performed critical revision of the manuscript. All authors read and approved the final manuscript.

Competing interests

The authors declare no competing interests.

Additional information

Supplementary Information The online version contains supplementary material available at <https://doi.org/10.1038/s41598-022-12938-3>.

Correspondence and requests for materials should be addressed to A.M. or W.Y.L.

Reprints and permissions information is available at www.nature.com/reprints.

Publisher's note Springer Nature remains neutral with regard to jurisdictional claims in published maps and institutional affiliations.



Open Access This article is licensed under a Creative Commons Attribution 4.0 International License, which permits use, sharing, adaptation, distribution and reproduction in any medium or format, as long as you give appropriate credit to the original author(s) and the source, provide a link to the Creative Commons licence, and indicate if changes were made. The images or other third party material in this article are included in the article's Creative Commons licence, unless indicated otherwise in a credit line to the material. If material is not included in the article's Creative Commons licence and your intended use is not permitted by statutory regulation or exceeds the permitted use, you will need to obtain permission directly from the copyright holder. To view a copy of this licence, visit <http://creativecommons.org/licenses/by/4.0/>.

© The Author(s) 2022